ARTICLES

$^3H(p,\gamma)^4He$ cross section

K. I. Hahn, C. R. Brune, and R. W. Kavanagh
W. K. Kellogg Radiation Laboratory, 106-38, California Institute of Technology, Pasadena, California 91125
(Received 29 August 1994)

The absolute differential cross section for the $^3H(p,\gamma)^4He$ reaction was measured for $0.1 \leq E_p \leq 6.0$ MeV. Gamma rays produced by proton bombardment of Ti-^3H targets were detected simultaneously with BGO and NaI scintillators positioned at 90° with respect to the incident beam. Our results are higher than the most recently reported (p,γ) data, but in good agreement with all other previous (p,γ) experiments. The present results support the $^4He(\gamma,p)$ cross sections recommended by Calarco *et al.* in their discussions of the charge asymmetry of the nuclear force in ^4He.

PACS number(s): 25.40.Lw, 27.10.+h

I. INTRODUCTION

Comparisons of the cross sections for the $^3H(p,\gamma)^4He$, $^3He(n,\gamma)^4He$, $^4He(\gamma,p)^3H$, and $^4He(\gamma,n)^3He$ reactions have led to suggestions of charge-symmetry breaking in the nuclear force. The ratio of the photonucleon cross sections, $R_\gamma = \sigma_{\gamma,p}/\sigma_{\gamma,n}$, for the ^4He system gives valuable information, as conventional theoretical models [1–5] without charge-symmetry breaking predict $R_\gamma \approx 1.1$ for $E_\gamma = 25$–40 MeV. Calarco *et al.* [6] examined all of the experimental results available in 1983 and recommended $R_\gamma \approx 1.7$–1.4 for $E_\gamma = 25$–30 MeV, hence suggesting the strong possibility of nonzero charge asymmetry in the nuclear force. Their recommended $^4He(\gamma,p)^3H$ cross section was based heavily on the inverse $^3H(p,\gamma)^4He$ data for $E_\gamma \lesssim 38$ MeV because of the agreement among all the capture results [7–12]. However, it agrees with only some of the $^4He(\gamma,t)^1H$ results [13–15], and is higher than other phototriton results [16–18] below $E_\gamma = 31$ MeV. For the $^4He(\gamma,n)^3He$ cross section, Calarco *et al.* primarily used the experimental results by Berman *et al.* [19] and Ward *et al.* [20], which are in agreement with some of the earlier data [21–23], although other measurements [14,24–26] are substantially larger near 25 MeV. The situation was also unclear because all of the experiments that measured both photonucleon reactions simultaneously gave $R_\gamma \sim 1.0$ [13,17], in disagreement with Calarco *et al.* Since then, there have been more measurements of the cross sections for the (p,γ), (γ,p), (n,γ), and (γ,n) reactions, seeking to resolve the discrepancies among the earlier experiments (see Ref. [27] for reviews of these experiments).

Prior to Calarco *et al.*'s studies in 1983, there was relatively little disagreement among different $(\gamma,p)/(p,\gamma)$ experiments. In 1988, Bernabei *et al.* [28] reported cross sections for the $^4He(\gamma,p)$ reaction at $E_\gamma = 28.6$–58.1 MeV, using a monoenergetic photon beam and a $\sim 4\pi$ proton detector, with results substantially lower than the $\sigma_{\gamma,p}$ values recommended by Calarco *et al.* Furthermore, recent $^3H(p,\gamma)$ results by Feldman *et al.* [29] are $\sim 35\%$ lower than the earlier capture experiments and agree with the results of Bernabei *et al.* If these two experiments are compared with the recommended values for $\sigma_{\gamma,n}$, the ratio R_γ by Bernabei *et al.* is 1.01 ± 0.06 for $E_\gamma = 28.6$–42.4 MeV and the ratio R_γ by Feldman *et al.* is 1.09 ± 0.17 for $E_\gamma = 24$–31 MeV. Hence, these new results suggest no need for charge-symmetry breaking. However, the most recent measurement of the $^4He(\gamma,p)$ cross section by Van Hoorebeke *et al.* [30], using 34-MeV end-point bremsstrahlung photons and proton detectors at nine angles, is yet in disagreement with the results of Bernabei *et al.* and Feldman *et al.*, but is in perfect agreement with the values previously recommended by Calarco *et al.* Thus, $\sim 35\%$ discrepancies in the $^3H(p,\gamma)$ cross section remain unsettled.

In this paper, we report new measurements of the $^3H(p,\gamma)$ cross section for $0.1 \leq E_p \leq 6.0$ MeV, with results that support the values recommended by Calarco *et al.*

II. EXPERIMENT AND DATA ANALYSIS

A. Introduction

The experiment was performed using 0.4–20 μA proton beams with energies up to the 6-MeV limit of the Caltech Pelletron Tandem. The molecular ions H_2^+ and H_3^+ from the terminal ion source were used to provide low beam energies, $0.2 \leq E_p \leq 0.5$ MeV and $E_p = 0.1$ MeV, respectively. The γ rays from the $^3H(p,\gamma)$ reaction were measured simultaneously with a 5.08-cm-length × 5.08-cm-diam BGO detector and a 7.62-cm-length × 7.62-cm-diam NaI detector. The detectors were positioned at the opposite sides of the target and at 90° with respect to the incident beam, as shown schematically in Fig. 1. The distance between the center of the target and the front aluminum surface of each detector was 10.2 cm for the

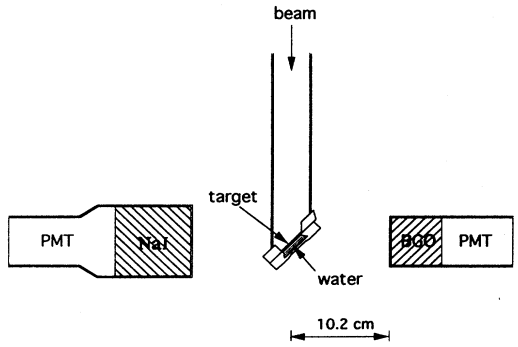

FIG. 1. Schematic of the experimental setup, showing the target and the NaI and BGO detectors.

^{3}H(p,γ) measurements with $1.0 \leq E_p \leq 6.0$ MeV and 3.1 cm for $0.1 \leq E_p \leq 1.0$ MeV.

Two Ti-^{3}H targets were used in this work, one with a Ti-^{3}H layer on a 31.7-mm-diam Ta (0.76-mm thickness) backing and the other on a 31.7-mm-diam Cu (0.81-mm thickness) backing. The targets were mounted with $\theta_{tgt} = 45°$ with respect to the incident beam and were water cooled. The ^{3}H areal densities ($\pm 3\%$) of 1.15×10^{18} ^{3}H atoms/cm^2 and 3.80×10^{17} ^{3}H atoms/cm^2 for the Ta-backing target and the Cu-backing target, respectively, were measured using the ^{3}H(d,α) reaction. (The Ti areal densities were determined to be 1.35×10^{18} Ti atoms/cm^2 and 2.16×10^{17} Ti atoms/cm^2 for the Ta-backing target and the Cu-backing target, respectively, by elastic α scattering.) Details of the target preparation and surface-density measurements have been described elsewhere [31].

In order to determine the absolute ^{3}H(p,γ)^{4}He cross section, it is important to determine accurate efficiencies for the detectors. Due to the lack of practical radioisotope sources or reactions that can be used to determine the intrinsic efficiencies of the BGO and NaI detectors for high-energy γ rays ($E_\gamma > 20$ MeV), we used the Monte Carlo program EGS4 [32] to obtain the absolute detection efficiencies. Since this program simulates the behaviors of γ rays, electrons, and positrons based on knowledge of the probabilities for bremsstrahlung production, photoelectric absorption, Compton scattering, pair production, energy loss, and other physical processes over a wide range of energies, it is expected to calculate detection efficiencies very accurately at any energy. A recent experiment by Mao *et al.* [33] used EGS4 for the detection efficiency of a NaI detector and showed that the EGS4 calculation accurately reproduced measurements taken with a calibrated ^{152}Eu source and using the ^{9}Be($\alpha,d\gamma$)^{11}B reaction. We have checked the program for the case of bare BGO and NaI crystals and isotropic point γ-ray sources with various energies up to 30 MeV, for which the total detection efficiencies were reproduced (within 2%) by analytical calculation. We have also used the ^{19}F($p,\alpha\gamma$)^{16}O reaction in an independent test of EGS4 (described below), incorporating the geometry and material of the present experiments. Since the penetration of 6-MeV γ rays is somewhat greater than that of 20–24 MeV γ rays, this test should sample all of the materials of our detection system.

B. Test of EGS4 with the ^{19}F($p,\alpha\gamma$)^{16}O reaction

1. *Introduction*

Because we depend exclusively on our Monte Carlo calculations for the γ-detection efficiencies, it is important to test the Monte Carlo program. We used the ^{19}F($p,\alpha\gamma$)^{16}O reaction at the $E_p = 340$ keV resonance, which yields a nearly monochromatic 6.13-MeV γ ray (96.9%) from the α_2 transition. The α yield is known to be isotropic in the center-of-mass system within an accuracy of 2% [34]. The γ yield is slightly anisotropic [35]: $W(\theta) = 1 - (0.0346 \pm 0.0013)\cos^2\theta$, but the anisotropy is ignored in the analysis. The absolute measurement of the α yield from the ^{19}F($p,\alpha\gamma$)^{16}O reaction depends only on geometrical conditions that can be measured accurately, since the intrinsic efficiency of the α detector is almost unity. Hence, by comparing the absolute yields of α particles and γ rays from the ^{19}F($p,\alpha\gamma$)^{16}O reaction, we can measure the γ-ray detection efficiency, which, in turn, can be compared to Monte Carlo calculations.

2. *The α yield from the ^{19}F($p,\alpha\gamma$)^{16}O reaction*

A ~ 50-μg/cm^2 CaF_2 film evaporated on a 0.76-mm-thick Ta backing (at $\theta_{tgt} = 45°$) was bombarded with 347-keV protons in a scattering chamber. The α particles from the ^{19}F($p,\alpha\gamma$)^{16}O reaction were detected by a Si(SB) detector at $\theta_{lab} = 165°$, with a 3.43-mm-diam aperture at 8.69 cm from the target, yielding a solid angle of 1.22×10^{-3} sr in the laboratory frame. In order to stop most of the elastic protons, a 3.05-μm Mylar window was placed behind the collimator in front of the detector. The dead time of the multichannel analyzer (MCA)

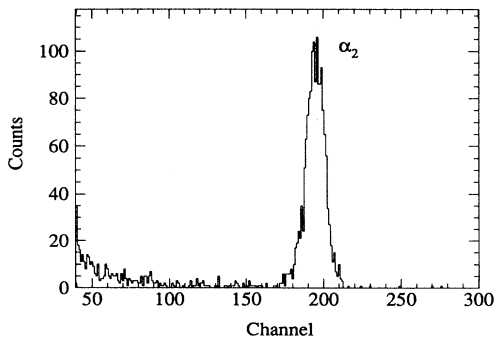

FIG. 2. The Si-detector spectrum from the ^{19}F($p,\alpha\gamma$)^{16}O reaction, showing the α_2 group cleanly separated from background in lower channels.

and counts from the current integrator were recorded for each run. We changed beam-focusing conditions as well as target positions and found no evidence (within 2%) for nonuniformity of the target.

Figure 2, a measurement with the CaF_2 side of the target, shows the α_2 group clearly separated from background in lower channels. A measurement with the Ta side revealed no background counts for our α measurement. To obtain the γ-detection efficiencies of BGO and NaI, we do not need to know the target thickness since we used the same target with $\theta_{\rm tgt} = 45°$ and beam energies that are essentially on the plateau of the thick-target yield for both α- and γ-yield measurements.

For the absolute α yield per proton per steradian, we have

$$Y_\alpha = \frac{N_\alpha}{n_p \, \Delta\Omega_{\rm c.m.}} , \quad (1)$$

where N_α is the number of α particles, n_p is the number of protons incident on the target, and $\Delta\Omega_{\rm c.m.}$ is the detector solid angle in the center-of-mass frame. We obtained the α yield, $Y_\alpha = 9.02 \pm 0.34 \times 10^{-10}$, where the error is from a 2.5% statistical error of the total α counts, a 1% error in the beam current, a 1% error in the solid angle, and a 2% error for possible nonisotropy.

3. The γ yield from the $^{19}F(p,\alpha\gamma)^{16}O$ reaction

The γ rays from the same CaF_2 target were detected under the identical experimental setup as that for the $^3H(p,\gamma)$ experiment: the target was mounted at 45° with respect to the beam, was water cooled, and the BGO and NaI detectors were positioned at 90° to the beam.

The top and bottom spectra in Fig. 3 show the (background-subtracted) experimental data (triangles) of the BGO detector and the NaI detector, respectively, positioned at 10.2 cm from the target center. The known γ energies from an AmBe source and natural background lines were found to be linear with MCA channels and were used for energy calibration. Using EGS4, 5×10^6 events of the 6.13-MeV γ rays from the 6 mm × 17 mm target area were generated isotropically. The total number of γ rays and their energies deposited in the BGO and NaI crystals were calculated. The three-dimensional geometry of all the absorbers (e.g., the target holder and the surroundings of the crystals) and their materials were carefully determined and used in EGS4. Since the Monte Carlo program assumes perfect detector resolution, the Monte Carlo spectra were convolved with energy resolutions of 4% and 5% (FWHM of the Gaussian distribution) for BGO and NaI, respectively, to fit the shapes of the experimental data. The Monte Carlo simulations (histograms) and the experimental data (triangles) agree almost perfectly. The yield of the γ rays per proton per steradian is

$$Y_\gamma = \frac{N_\gamma}{n_p 4\pi t_{\rm eff}} , \quad (2)$$

where N_γ is the number of counts in a selected energy cut between 4 and 6.5 MeV, n_p is the number of incident protons, and $t_{\rm eff}$ is the total absolute detection efficiency determined from EGS4 for the same energy cut used for N_γ. The systematic error in $t_{\rm eff}$ calculated by the Monte Carlo simulation is estimated to be ±6%, which is mainly due to the uncertainties in the detector position, the energy calibration, and the line shape. For example, a 2% error in the detector distance in EGS4 changes the final $t_{\rm eff}$ result as much as 3% due mainly to changes in solid angle. The combined uncertainty in the energy calibration and the line shape also introduces 3% errors in the $t_{\rm eff}$ values. Two extreme cases of energy cuts, the 5–6.5 MeV cut and the 1–6.5 MeV cut, in Fig. 3 agree within 2%. This indicates the linearity of the detector response as well as the quality of the Monte Carlo simulation.

The γ yields for the BGO and NaI detectors at 10.2 cm from the target were determined to be $9.01 \pm 0.60 \times 10^{-10}$ and $9.51 \pm 0.60 \times 10^{-10}$, respectively, which are in good agreement with the α yield of $9.02 \pm 0.34 \times 10^{-10}$. More extensive tests were done to verify that the EGS4 calculations are consistent with different experimental configurations. The experiments were tested with detectors at several different positions: (a) detectors at 10.2 cm, (b) detectors exchanged at 10.2 cm, (c) detectors at 15.2 cm, and (d) detectors exchanged at 15.2 cm. Table I shows

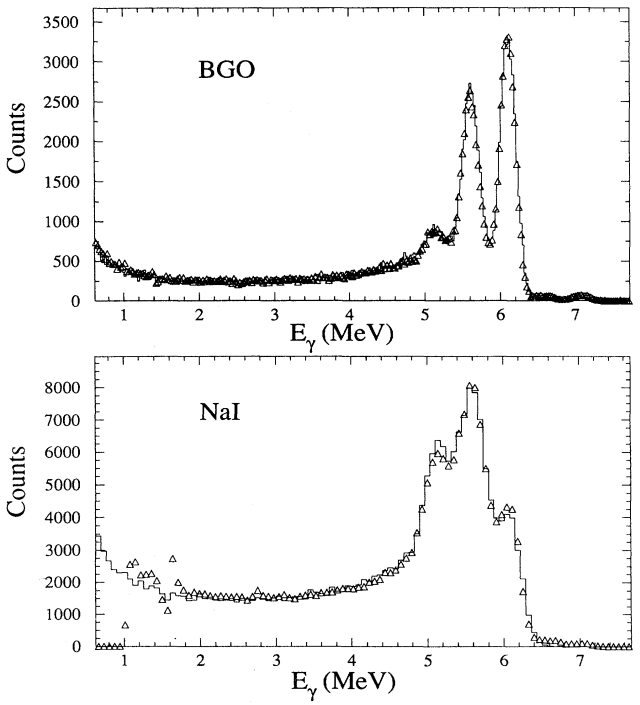

FIG. 3. The experimental (triangles) and the Monte Carlo (histograms) spectra for the $^{19}F(p,\alpha\gamma)^{16}O$ reaction are compared. The energy spectra from the Monte Carlo simulations were smeared with ~ 4% and ~ 5% energy resolutions to match the experimental data of the BGO and NaI detectors, respectively.

TABLE I. The absolute yields of 6.13-MeV γ rays and α particles from the ^{19}F$(p,\alpha_2\gamma)^{16}$O reaction, per proton per steradian.

Detector positions		$Y_\gamma \times 10^{10}$ BGO	$Y_\gamma \times 10^{10}$ NaI	$Y_\alpha \times 10^{10}$
Si(SB) detector at $\theta_{lab} = 165°$		—	—	9.02±0.34
BGO at −10.2 cm	NaI at +10.2 cm[a]	9.01±0.60	9.51±0.60	—
BGO at +10.2 cm	NaI at −10.2 cm	9.01±0.59	9.41±0.57	—
BGO at −15.2 cm	NaI at +15.2 cm	8.89±0.58	9.60±0.61	—
BGO at +15.2 cm	NaI at −15.2 cm	9.09±0.61	9.76±0.61	—

[a]The same detector position used for the ^{3}H$(p,\gamma)^4$He reaction at $E_p \geq 1.0$ MeV.

the γ yields from the different detector positions. The results indicate that the absolute efficiencies obtained using EGS4 are consistent, in agreement within errors among themselves and also with the α result.

However, there is an obvious trend that the NaI values are consistently a few percent higher than the BGO values. We also observed this effect in the ^{3}H$(p,\gamma)^4$He experiment. This cannot be caused entirely by using the wrong geometrical conditions in the Monte Carlo calculations, because exchanging the detectors at both 10.2 cm and 15.2 cm also shows these effects. There are several other possibilities that might cause these effects, for example, slightly damaged crystals or wrong dimensions of the materials inside the aluminum housings. Our conservative estimate of ±6% error in determining the efficiencies should be sufficient to cover these systematic errors. Because a subsequent test with two supposedly identical NaI detectors for the ^{3}H(p,γ) experiment gave ~ 5% different results, we conclude that these slight deviations are possible among different detectors, not because of any fundamental problems with the Monte Carlo program.

We have done many careful tests on the Monte Carlo EGS4 program by comparing the γ yields to the α yields from the ^{19}F$(p,\alpha\gamma)^{16}$O reaction. The two different detector systems also allow us to crosscheck the γ yields and the results agree within 6%. We conclude that the Monte Carlo simulations successfully predict the detection efficiencies and will be used in the calculation of the ^{3}H$(p,\gamma)^4$He cross section.

C. Data analysis of the ^{3}H$(p,\gamma)^4$He experiment

We used a Ti-^{3}H target on a Ta backing for the ^{3}H$(p,\gamma)^4$He reaction at beam energies between 0.1 and 6.0 MeV. As the proton beam energy increases, the neutron background from the (p,n) reaction with ^{3}H, Ti, and Ta increases in energy and intensity. Therefore, our highest beam energy run at $E_p = 6.00$ MeV, which was the maximum proton energy allowed by the accelerator, was used to check the background in the high-energy region where we expect to have only the γ rays from the ^{3}H$(p,\gamma)^4$He reaction. The top spectra in Figs. 4 and 5 show the (cosmic-ray background-subtracted) experimental data (histograms) and the Monte Carlo simulations (dotted curves) of the BGO and NaI detectors, respectively, for the ^{3}H$(p,\gamma)^4$He reaction at E_p = 6.00 MeV. The Monte Carlo simulations agree with the experimental data perfectly in the high-energy region. However, the huge excess yields in the experimental data in the low-energy region are due to the natural γ-ray background and neutrons from ^{3}H and Ti in the target and the Ta backing. Because the Q value of the ^{3}H(p,γ) reaction, 19.8 MeV, is considerably higher than the Q values of the ^{181}Ta(p,γ) and ^{48}Ti(p,γ) reactions, 7.09 MeV and 6.76 MeV, respectively, the high-energy

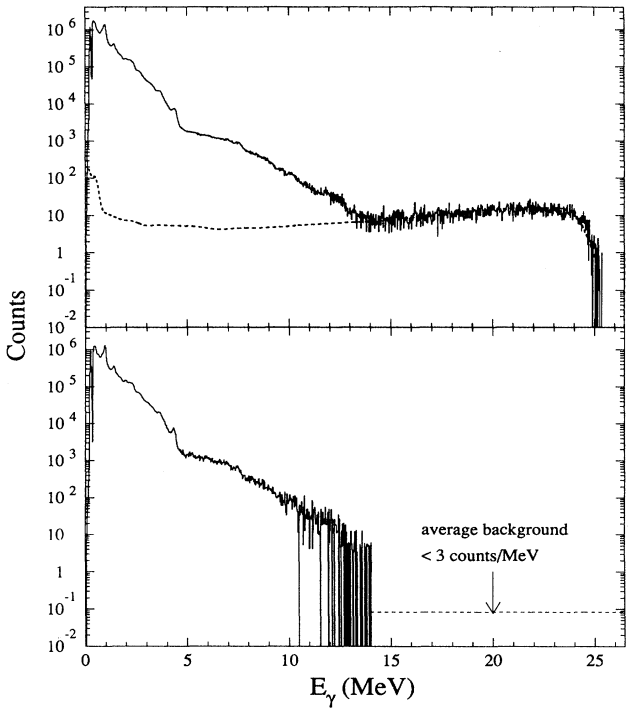

FIG. 4. The top spectrum shows the experimental data (histogram) and the Monte Carlo result (dotted curve) of the BGO detector for the ^{3}H(p,γ) reaction at $E_p = 6.0$ MeV using a Ti-^{3}H target on a Ta backing. The bottom spectrum is from a background run using a Ti target on a Ta backing, normalized to the same integrated charge as the top spectrum. The dotted line in the $E_\gamma \geq 14$ MeV region indicates negligible background for the γ rays with $E_\gamma \geq 14$ MeV from ^{3}H in the top spectrum.

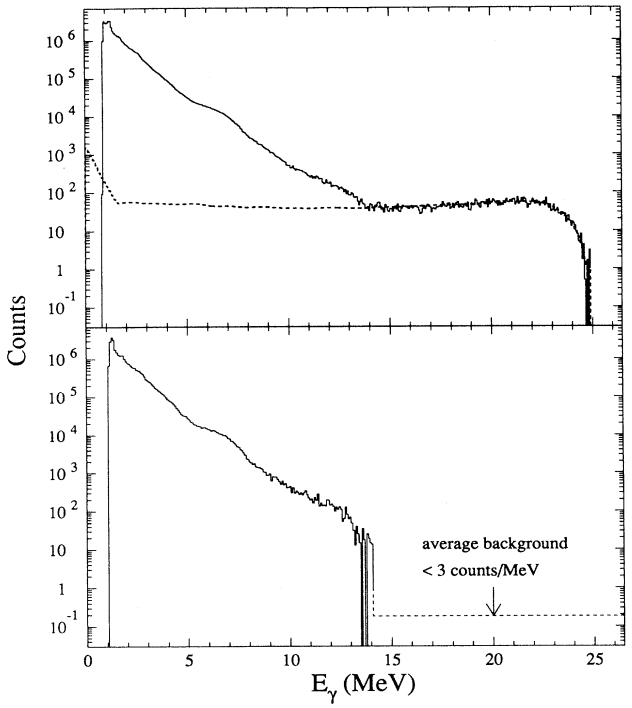

FIG. 5. Spectra from the NaI detector obtained during the same runs as in Fig. 4.

γ rays from ^{3}H are cleanly separated from those from other target materials. The bottom spectra in Figs. 4 and 5 show the (cosmic-ray background-subtracted) experimental data using only a Ti target on a Ta backing, having the same thickness of Ti as the Ti-^{3}H target, and indicate negligible background in the high-energy region.

We measured the γ rays from the ^{3}H$(p,\gamma)^4$He reaction without changing any experimental conditions (except, obviously, the target and the beam energy) of the ^{19}F$(p,\alpha\gamma)^{16}$O experiment. Hence, we utilized the same geometrical inputs that were used successfully in EGS4 to calculate the total detection efficiency for the ^{19}F$(p,\alpha\gamma)^{16}$O experiment. Perry and Bame [12] found that the angular distributions of the ^{3}H$(p,\gamma)^4$He reaction have the form

$$W(\theta_{\rm c.m.}) = (\sin\theta_{\rm c.m.} + a\sin\theta_{\rm c.m.}\cos\theta_{\rm c.m.})^2 , \qquad (3)$$

where a is the asymmetry coefficient. The asymmetry coefficient is approximately a linear function of proton energy, $a = 0.01 + 0.02\,E_p$, where E_p is in MeV (see Refs. [10,12]). In the Monte Carlo calculations, for the given proton energy, the γ-ray angle in the center-of-mass system was weighted according to Eq. (3), and then the angle and the energy of the γ ray in the laboratory system were calculated using relativistic kinematics, correcting for recoil energy and Doppler shift. For each proton-energy run, 1 000 000 γ-ray emissions from the target were simulated and their energies deposited in the BGO and NaI crystals were determined. As shown in Figs. 4 and 5, the Monte Carlo simulations do not agree with the experimental data for the γ rays with energies below a certain cutoff energy due to the neutron background. Hence, the number of γ rays, N_γ, above a cutoff energy is used to calculate the total cross section of the ^{3}H$(p,\gamma)^4$He reaction using the expression

$$\sigma_{\rm tot} = \frac{N_\gamma}{n_p\, N_t\, t_{\rm eff}} , \qquad (4)$$

where n_p is the number of protons that passed through the tritium target, N_t is the areal density of tritons, and $t_{\rm eff}$ is the total detection efficiency of the γ rays with deposited energies higher than the same cutoff energy used for N_γ. With the angular distribution of the γ rays from Eq. (3), the differential cross section can be expressed by

$$\frac{d\sigma}{d\Omega} = \frac{\sigma_{\rm tot} W(\theta)}{\int W(\theta) d\Omega} . \qquad (5)$$

The experimental data were corrected for cosmic-ray background (< 5%), spectra for which were collected frequently during the experiment. Figures 6 and 7 show the (room background-subtracted) experimental γ spectra of BGO and NaI, respectively, from the ^{3}H$(p,\gamma)^4$He reaction at 0.1, 1.0, and 6.0 MeV, with the Ti-^{3}H target on Ta

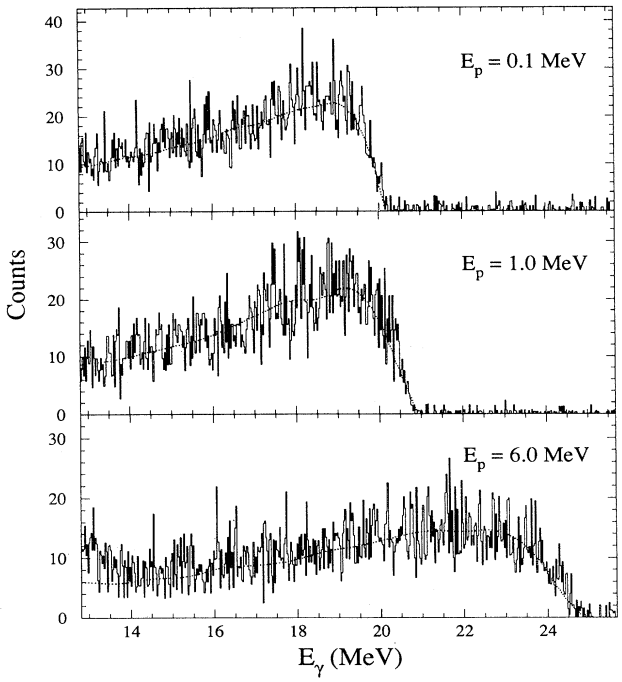

FIG. 6. BGO γ-ray spectra from the ^{3}H(p,γ) reaction with the Ta-backed target at three different beam energies, 0.1, 1.0, and 6.0 MeV. The histograms are the experimental data and the dotted curves are the Monte Carlo simulations used to calculate the total detection efficiencies. Excess counts in the experimental data in low-energy regions in Figs. 6–9 are due to neutrons, as explained in text, and are not used for the efficiency calculations.

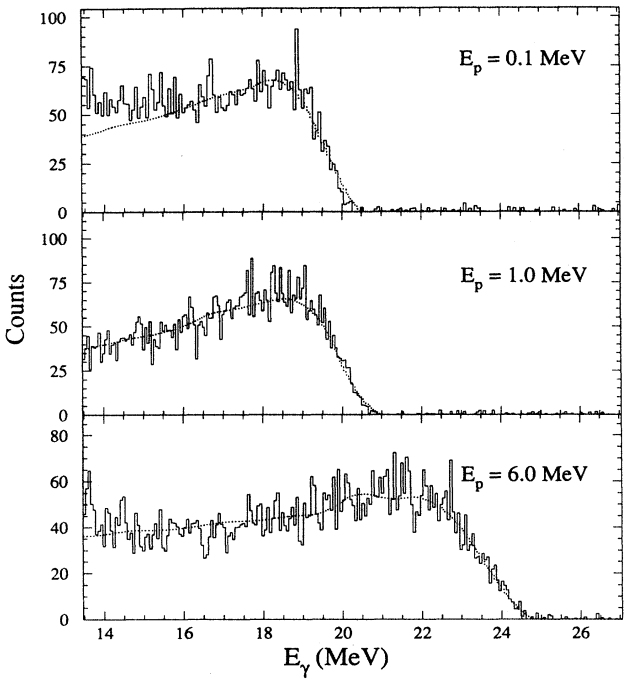

FIG. 7. NaI γ-ray spectra obtained during the same runs as in Fig. 6.

backing. The experimental data (histograms) are accurately reproduced by the Monte Carlo simulations (dotted curves), which in turn give t_{eff} for the cross-section determination.

The Monte Carlo results were convolved with energy resolutions of 4% and 5% for BGO and NaI, respectively, to optimize agreement with the experimental data. The structures in the dotted curves are not significant as they are due to statistical fluctuations. The statistical error in t_{eff} is less than 1% due to the large number of events (10^6) used in EGS4. As explained in the previous section, the systematic uncertainty in t_{eff} calculated by the Monte Carlo simulation is estimated to be ±6%. During the (p,γ) measurements, the proton beam was rastered over ~ 1 cm^2 of the targets, which were water cooled. From many repeated measurements at $E_p = 1$ MeV throughout the experiment, the targets proved stable, less than 3% loss during the course of our experiment. The uncertainty in the tritium-target areal density is ±3%.

Unfortunately, some gain shifts (< 4%) were observed in our NaI spectra, associated with high counting rates. The gain-shift effects were important only for the higher proton energies, where the counting rate is primarily from the neutron flux. They also affected the analysis, as the Monte Carlo simulations required a larger resolution to match the experimental spectra. The runs with proton energies < 4 MeV showed negligible gain shifts. The runs with gain shifts resulted in larger errors in our measurements of the cross sections as shown in Table II.

At lower beam energies with smaller yields from the ^{3}H(p,γ)^{4}He reaction, the two detectors were moved closer to the target (3.1 cm for the runs with $E_p \leq$ 1.00 MeV). The results with $E_p = 1.0$ MeV measured at both 10.2 and 3.1 cm were used to normalize the results for $E_p \leq 0.75$ MeV. To correct for proton energy loss in the target, the effective energy assigned to each run was the average energy in the target, as listed in Table II. Systematic errors in the cross sections due to uncertainty in the energy loss of the proton beam are estimated to be 2% for the 0.5–0.75 MeV runs and 5%

TABLE II. The differential cross section of the ^{3}H(p,γ)^{4}He reaction at $\theta = 90°$.

	Ta backing			Cu backing		
		BGO	NaI		BGO	NaI
E_p (MeV)	$\bar{E}_p$[a] (MeV)	$\left(\frac{d\sigma}{d\Omega}\right)_{\theta=90°}$ (μb/sr)	$\left(\frac{d\sigma}{d\Omega}\right)_{\theta=90°}$ (μb/sr)	$\bar{E}_p$[a] (MeV)	$\left(\frac{d\sigma}{d\Omega}\right)_{\theta=90°}$ (μb/sr)	$\left(\frac{d\sigma}{d\Omega}\right)_{\theta=90°}$ (μb/sr)
0.100	0.0668	0.142±0.016[b]	0.156±0.018[b]	0.0936	0.225±0.029[b]	0.245±0.030[b]
0.200	0.172	0.513±0.058[b]	0.507±0.058[b]	0.195	0.591±0.077[b]	0.609±0.072[b]
0.300	0.277	0.881±0.098[b]	0.838±0.096[b]	0.296	0.957±0.12[b]	1.02±0.12[b]
0.500	0.483	1.48±0.12[b]	1.54±0.13[b]	0.497	1.60±0.16[b]	1.70±0.14[b]
0.750	0.736	2.25±0.19[b]	2.23±0.18[b]	0.747	2.39±0.24[b]	2.53±0.22[b]
1.00	0.988	3.01±0.21	3.16±0.21	0.998	3.09±0.21	3.37±0.23
1.50				1.50	4.55±0.34	5.13±0.36
2.00	1.99	6.27±0.43	6.63±0.46	2.00	6.20±0.42	6.84±0.47
2.50	2.49	7.41±0.51	7.91±0.54	2.50	7.14±0.49	7.29±0.73[c]
3.00	2.99	8.41±0.58	9.07±0.63			
3.50	3.49	8.93±0.63	9.74±0.67			
4.00	4.00	9.35±0.64	10.4±1.0[c]			
4.50	4.50	9.44±0.65	10.0±1.0[c]			
5.00	5.00	9.28±0.64	10.1±1.0[c]			
5.50	5.50	9.07±0.63	9.39±0.94[c]			
6.00	6.00	8.94±0.63	9.95±0.99[c]			

[a]Average beam energy in the target.
[b]Errors due to the energy loss in the target are included.
[c]Errors due to the gain shift problems as explained in text are estimated to be ~10%.

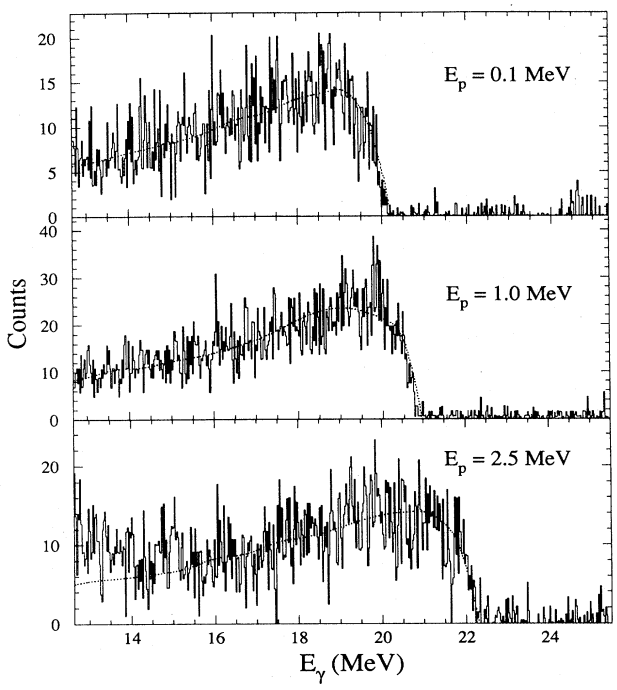

FIG. 8. BGO γ-ray spectra from the ^{3}H(p,γ) reaction with the Cu-backed target at three different beam energies, 0.1, 1.0, and 2.5 MeV. The histograms are the experimental data and the dotted curves are the Monte Carlo simulations used to calculate the total detection efficiencies.

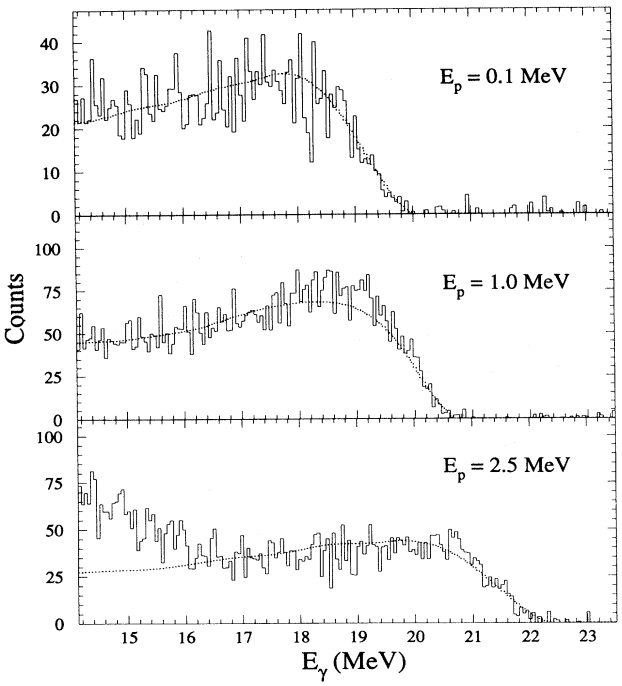

FIG. 9. NaI γ-ray spectra for the same runs as in Fig. 8.

for the 0.1–0.3 MeV runs, and are included in the total errors. Using Eq. (4) with the total detection efficiency calculated by EGS4 and Eq. (5), the results for the differential cross sections at $\theta = 90°$ are listed in Table II.

We have also carried out the ^{3}H$(p,\gamma)^4$He experiment with the Ti-^{3}H target on the Cu backing. The neutron threshold of Cu at $E_p = 2.1$ MeV prevented measurement of the ^{3}H$(p,\gamma)^4$He reaction at energies higher than 2.5 MeV. Figures 8 and 9 show the spectra at three different beam energies, 0.1, 1.0, and 2.5 MeV. The results for the differential cross sections using this target are also listed in Table II.

III. DISCUSSION

The results for the ^{3}H(p,γ) cross sections are listed in Table II and the results with the Ta-backed target are shown in Fig. 10. Our results using Ta and Cu backings agree well. Although our NaI results and BGO results agree within errors, the NaI results are consistently $\sim 6\%$ higher than the BGO results for $1.0 \leq E_p \leq 6.0$ MeV. This effect was also evident in our tests of the Monte Carlo results using the ^{19}F$(p,\alpha\gamma)^{16}$O reaction, although both BGO and NaI results agreed with the α-detection results within errors. We later replaced our NaI detector by another supposedly identical NaI detector without changing any experimental conditions; the new NaI results are $\sim 5\%$ lower, in better agreement with the BGO data.

Shown in Fig. 10 are four previous (p,γ) cross-

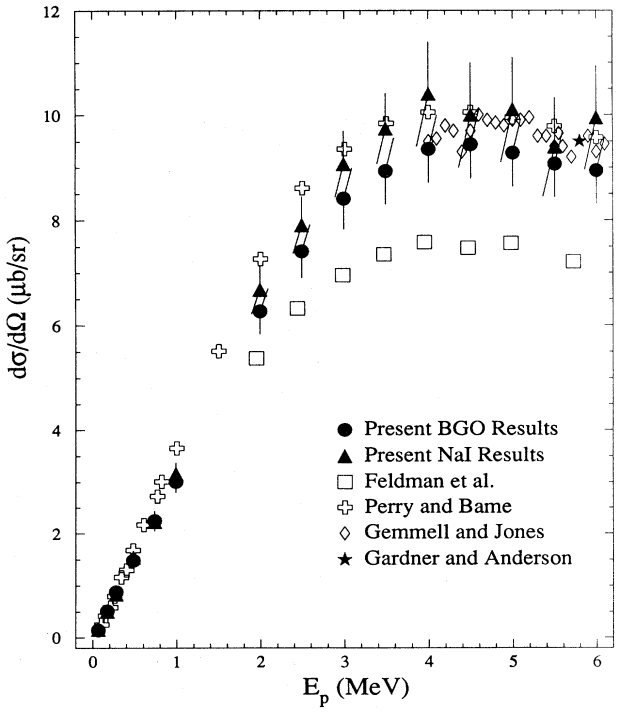

FIG. 10. Differential cross section for the ^{3}H$(p,\gamma)^4$He reaction at $\theta_{\rm lab} = 90°$.

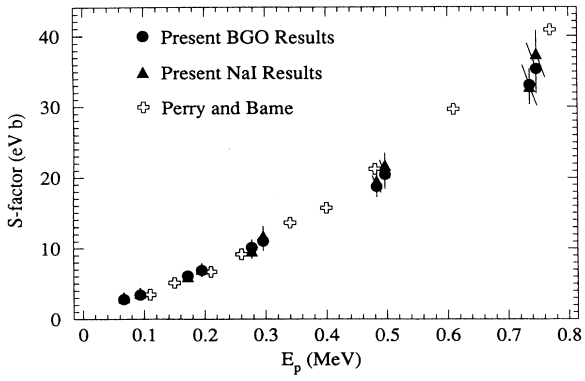

FIG. 11. S factors for the ^{3}H(p,γ)^{4}He reaction for $E_p \leq 0.75$ MeV.

section measurements at proton energies between 0.1 and 6.0 MeV. (The results of Meyerhof *et al.* are not shown, since they were normalized to those of Perry and Bame; however, they confirm the shape of σ vs E above 3 MeV.) The experimental data fall into two distinct groups, with the data of Feldman *et al.* $\sim$ 35% lower than the others. Only our results used the Monte Carlo simulations, which were tested to be very accurate from the ^{19}F($p,\alpha\gamma$) reaction in the identical geometries, for the detection efficiencies. The total S factors ($= \sigma_{\rm tot} E e^{2\pi\eta}$ and $\eta = e^2 Z_1 Z_2/\hbar v$) at low proton energies are plotted in Fig. 11, and agree with the values of Perry and Bame, also plotted there. There is also considerable spread in theoretical calculations [1–5]. The most recent, by Sofianos *et al.* [36], is in fair agreement with the (p,γ) results of Feldman *et al.*, and with the ratio R_γ near unity.

IV. CONCLUSION

We have measured the absolute cross section of the ^{3}H(p,γ) reaction with an accuracy of $\pm 7\%$ for $0.1 \leq E_p \leq 6.0$ MeV, corresponding to photon energies $19.9 \leq E_\gamma \leq 24.3$ MeV. Our results are in agreement with the previous results of Refs. [10–12] and, by extrapolation, with the higher-energy (p,γ) results of McBroom *et al.* [8]; they disagree with the most recent (p,γ) results of Feldman *et al.* [29], whose lower values, combined with the (γ,n) cross sections recommended by Calarco *et al.*, indicated that no charge-symmetry violation in ^{4}He is required. The present results support the recommended (γ,p) cross sections given by Calarco *et al.*, and thus the maximum cross section of about 1.8 mb near $E_\gamma = 25$ MeV. Summed with their recommended (γ,n) cross section of 1.1 mb, the total, 2.9 mb, agrees closely with the direct measurements of Wells *et al.* [37]. However, the ratio $R_\gamma = 1.6$ then implies symmetry violation. Alternatively, taking the (γ,n) cross section to be $\sim$ 1.7 mb from the measurements of Refs. [24,38,39] fixes $R_\gamma \sim 1.1$, but conflicts with the measured sum.

ACKNOWLEDGMENT

This work was supported in part by the National Science Foundation, Grant No. PHY91-15574.

[1] M. Unkelbach and H. M. Hofmann, Nucl. Phys. **A549**, 550 (1992).
[2] F. C. Barker, Aust. J. Phys. **37**, 583 (1984).
[3] D. Halderson and R. J. Philpott, Phys. Rev. C **28**, 1000 (1983).
[4] A. H. Chung, R. G. Johnson, and T. W. Donnelly, Nucl. Phys. **A235**, 1 (1974).
[5] J. T. Londergan and C. M. Shakin, Phys. Rev. Lett. **28**, 1729 (1972).
[6] J. R. Calarco, B. L. Berman, and T. W. Donnelly, Phys. Rev. C **27**, 1866 (1983).
[7] J. R. Calarco, S. S. Hanna, C. C. Chang, E. M. Diener, E. Kuhlmann, and G. A. Fisher, Phys. Rev. C **28**, 483 (1983).
[8] R. C. McBroom, H. R. Weller, N. R. Roberson, and D. R. Tilley, Phys. Rev. C. **25**, 1644 (1982). Note that this work was stated in Ref. [29] to be superseded by the latter, although no specific flaw was identified.
[9] W. E. Meyerhof, M. Suffert, and W. Feldman, Nucl. Phys. **A148**, 211 (1970).
[10] C. C. Gardner and J. D. Anderson, Phys. Rev. **125**, 626 (1962).
[11] D. S. Gemmell and G. A. Jones, Nucl. Phys. **33**, 102 (1962).
[12] J. E. Perry, Jr. and S. J. Bame, Jr., Phys. Rev. **99**, 1368 (1955).
[13] W. R. Dodge and J. J. Murphy, II, Phys. Rev. Lett. **28**, 839 (1972).
[14] A. N. Gorbunov, Phys. Lett. **27B**, 436 (1968).
[15] G. D. Wait, S. K. Kundu, Y. M. Shin, and W. F. Stubbins, Phys. Lett. **33B**, 163 (1970).
[16] H. G. Clerc, J. R. Stewart, and R. C. Morrison, Phys. Lett. **18**, 316 (1965).
[17] F. Balestra, E. Bollini, L. Busso, R. Garfagnini, C. Guaraldo, G. Piragino, R. Scrimaglio, and A. Zanini, Nuovo Cimento A **38**, 145 (1977).
[18] Yu. M. Arkatov, P. I. Vatset, V. I. Voloshchuk, V. A. Zolenko, I. M. Prokhorets, and V. I. Chmil', Yad. Fiz. **19**, 1172 (1974) [Sov. J. Nucl. Phys. **19**, 598 (1974)].
[19] B. L. Berman, D. D. Faul, P. Meyer, and D. L. Olson, Phys. Rev. C **22**, 2273 (1980).
[20] L. Ward, D. R. Tilley, D. M. Skopik, N. R. Roberson, and H. R. Weller, Phys. Rev. C **24**, 317 (1981).
[21] B. L. Berman, S. C. Fultz, and M. A. Kelly, Phys. Rev. C **4**, 723 (1971).
[22] B. L. Berman, F. W. K. Firk, and C.-P. Wu, Nucl. Phys. **A179**, 791 (1972).
[23] J. D. Irish, B. L. Berman, R. G. Johnson, B. J. Thomas, K. G. McNeill, and J. W. Jury, in *Few Particle Problems in Nuclear Interaction*, edited by I. Slaus, S. A.

Moszkowski, R. P. Haddock, and W. T. H. van Oers (North-Holland, Amsterdam, 1972), p. 888.
[24] J. D. Irish, R. G. Johnson, B. L. Berman, B. J. Thomas, K. G. McNeill, and J. W. Jury, Can. J. Phys. **53**, 802 (1975).
[25] C. K. Malcolm, D. V. Webb, Y. M. Shin, and D. M. Skopik, Phys. Lett. **47B**, 433 (1973).
[26] Yu. M. Arkatov, P. I. Vatset, V. I. Voloshchuk, V. N. Gur'ev, and A. F. Khodyachikh, Ukr. Fiz. Zh. **23**, 1818 (1978).
[27] D. R. Tilley, H. R. Weller, and G. M. Hale, Nucl. Phys. **A541**, 1 (1992).
[28] R. Bernabei, A. Chisholm, S. d'Angel, M. P. De Pascale, P. Picozza, C. Schaerf, P. Belli, L. Casano, A. Incicchittie, D. Prosperi, and B. Girolami, Phys. Rev. C **38**, 1990 (1988).
[29] B. Feldman, M. J. Balbes, L. H. Kramer, J. Z. Williams, H. R. Weller, and D. R. Tilley, Phys. Rev. C **42**, R1167 (1990).
[30] L. Van Hoorebeke, R. Van de Vyver, V. Fiermans, D. Ryckbosch, C. Van den Abeele, and J. Dias, Phys. Rev. C **48**, 2510 (1993).
[31] C. R. Brune and R. W. Kavanagh, Nucl. Instrum. Methods A **343**, 415 (1994).
[32] W. R. Nelson, H. Hirayama, and D. O. Rogers, SLAC Report 265, 1985.
[33] Z. Q. Mao, R. B. Vogelaar, A. E. Champagne, J. C. Blackmon, R. K. Das, K. I. Hahn, and J. Yuan, Nucl. Phys. **A567**, 125 (1994).
[34] J. A. Van Allen and N. M. Smith, Jr., Phys. Rev. **59**, 501 (1941).
[35] Th. Retz-Schmidt, Z. Naturforsch. Teil A **13**, 833 (1958).
[36] S. A. Sofianos, H. Fiedeldey, and W. Sandhas, Phys. Rev. C **48**, 2285 (1993).
[37] D. P. Wells, D. S. Dale, R. A. Eisenstein, F. J. Federspiel, M. A. Lucas, K. E. Mellendorf, A. M. Nathan, and A. E. O'Neill, Phys. Rev. C **46**, 449 (1992).
[38] R. E. J. Florizone, J. Asai, G. Feldman, E. L. Hallin, D. M. Skopik, and J. M. Vogt, Phys. Rev. Lett. **72**, 3476 (1994).
[39] S. I. Nagornyĭ, Yu. A. Kasatkin, V. A. Zolenko, I. K. Kirichendo, and A. A. Zayats, Yad. Fiz. **53**, 365 (1991) [Sov. J. Nucl. Phys. **53**, 228 (1991)].